Trigonometric-series solution for analysis of laminated composite beams

Trung-Kien Nguyen[a,*], Ngoc-Duong Nguyen[a], Thuc P. Vo[b], Huu-Tai Thai[c]

[a]*Faculty of Civil Engineering, Ho Chi Minh City University of Technology and Education, 1 Vo Van Ngan Street, Thu Duc District, Ho Chi Minh City, Vietnam*
[b]*Faculty of Engineering and Environment, Northumbria University, Newcastle upon Tyne, NE1 8ST, UK.*
[c]*School of Engineering and Mathematical Sciences, La Trobe University, Bundoora, VIC 3086, Australia.*

Abstract

A new analytical solution based on a higher-order beam theory for static, buckling and vibration of laminated composite beams is proposed in this paper. The governing equations of motion are derived from Lagrange's equations. An analytical solution based on trigonometric series, which satisfies various boundary conditions, is developed to solve the problem. Numerical results are obtained to compare with previous studies and to investigate the effects of length-to-depth ratio, fibre angles and material anisotropy on the deflections, stresses, natural frequencies and critical buckling loads of composite beams with various configurations.

Keywords: Trigonometric-series solution; Laminated composite beams; Static; Buckling; Vibration.

1. Introduction

Composite laminated beams have been increasingly used in the various engineering fields for example in constructions, spacecraft, aircraft, mechanical engineering, etc... In order to predict accurately their structural responses, various beam theories with different approaches have been developed. These beam theories can be divided into three following categories: classical beam theory (CBT), first-order beam theory (FBT) and higher-order theory (HBT). A general review and assessment of these theories for composite beams can be found in [1–3]. It should be noted that CBT is only suitable for thin beams due to neglecting shear effect. FBT overcomes this adverse by taking into account this effect. However practically an appropriate shear correction is required. By using higher-order variation of axial displacement, HBT predicts more accurate than CBT and FBT, and importantly no shear correction factor is necessary. Therefore, this theory has been increasingly applied in predicting responses of composite beams.

---

*Corresponding author, tel.: +848 3897 2092
Email address: kiennt@hcmute.edu.vn (Trung-Kien Nguyen)

For numerical methods, finite element method has been widely used to analyze composite beams [4–17]. For analytical approach, Navier solution is the simplest one, which is only applicable for simply supported boundary conditions ([18–20]). In order to deal with arbitrary boundary conditions, many researchers developed different methods. Ritz-type method is commonly used [21–24]. Khdeir and Reddy [25, 26] developed state-space approach to derive exact solutions for the natural frequencies and critical buckling loads of cross-ply composite beams. Chen et al. [27] also proposed an analytical solution based on state-space differential quadrature for vibration of composite beams. By using the dynamic stiffness matrix method, Jun et al. [28, 29] calculated the natural frequencies of composite beams based on third-order beam theory. A literature review shows that although Ritz procedure is efficient to deal with static, buckling and vibration problems of composite beams with various boundary conditions, the research on this interesting topic is still limited.

The objectives of this paper is to develop a new trigonometric-series solution for analysis of composite beams with arbitrary lay-ups. It is based on a higher-order theory which accounts for a higher-order variation of the axial displacement. By using Lagrange equations, the governing equations of motion are derived. Ritz-type analytical solution with new trigonometric series is developed for beams under various boundary conditions. The convergence and verification studies are carried out to demonstrate the accuracy of the proposed solution. Numerical results are presented to investigate the effects of length-to-depth ratio, fibre angle and material anisotropy on the deflections, stresses, natural frequencies and critical buckling loads of composite beams.

2. Theoretical formulation

A laminated composite beam with rectangular section ($b \times h$) and length L as shown in Fig. 1 is considered. It is made of n plies of orthotropic materials in different fibre angles with respect to the x-axis.

2.1. Kinetic, strain and stress relations

The displacement field of refined higher-order deformation theory ([30–32]) is given by:

$$u_1(x, z) = u_0(x) - zw_{0,x} + \left(\frac{5z}{4} - \frac{5z^3}{3h^2}\right)\phi_0(x) = u_0(x) - zw_{0,x} + \Psi(z)\phi_0(x) \qquad (1a)$$

$$u_3(x, z) = w_0(x) \qquad (1b)$$

where u_0, ϕ_0 and w_0 are unknown mid-plane displacements of beam; Ψ **is the shape function representing a higher-order variation of axial displacement**; the comma indicates partial differentiation with respect to the coordinate subscript that follows.

The strain field of beams is given by:

$$\epsilon_{xx}(x,z) = u_{0,x} - zw_{0,xx} + \Psi(z)\phi_{0,x} = \epsilon_x^0 + z\kappa_x^b + \Psi(z)\kappa_x^s \tag{2a}$$

$$\gamma_{xz}(x,z) = \Psi_{,z}\phi_0 = g(z)\phi_0 \tag{2b}$$

where ϵ_x^0 and κ_x^b, κ_x^s are the axial strain and curvatures of the beam.

The stress of the kth-layer is given by:

$$\sigma_{xx}^{(k)}(x,z) = \bar{Q}_{11}^{(k)}\left[\epsilon_x^0(x) + z\kappa_x^b(x) + \Psi(z)\kappa_x^s(x)\right] \tag{3a}$$

$$\sigma_{xz}^{(k)}(x,z) = \bar{Q}_{55}^{(k)}\gamma_{xz}(x,z) \tag{3b}$$

where $\bar{Q}_{11}^{(k)}$ and $\bar{Q}_{55}^{(k)}$ are the in-plane and out-of-plane elastic stiffness coefficients in the global coordinates (see [30] for details).

2.2. Variational formulation

The strain energy $\mathcal{U}$ of system is given by:

$$\begin{aligned}
\mathcal{U} &= \frac{1}{2}\int_V (\sigma_{xx}\epsilon_{xx} + \sigma_{xz}\gamma_{xz})dV \\
&= \frac{1}{2}\int_0^L \Big[A(u_{0,x})^2 - 2Bu_{0,x}w_{0,xx} + D(w_{0,xx})^2 + 2B^s u_{0,x}\phi_{0,x} - 2D^s w_{0,xx}\phi_{0,x} \\
&\quad + H^s(\phi_{0,x})^2 + A^s\phi_0^2\Big]dx
\end{aligned} \tag{4}$$

where (A, B, D, B^s, D^s, H^s) are the stiffnesses of laminated composite beams given by:

$$(A, B, D, B^s, D^s, H^s) = \sum_{k=1}^n \int_{z_k}^{z_{k+1}} (1, z, z^2, \Psi, z\Psi, \Psi^2)\bar{Q}_{11}^{(k)}bdz \tag{5}$$

$$A^s = \sum_{k=1}^n \int_{z_k}^{z_{k+1}} g^2\bar{Q}_{55}^{(k)}bdz \tag{6}$$

The work done $\mathcal{V}$ by the compression load N_0 and transverse load q is given by:

$$\mathcal{V} = \frac{1}{2}\int_0^L N_0(w_{0,x})^2 dx - \int_0^L qw_0 dx \tag{7}$$

The kinetic energy $\mathcal{K}$ of system is written by:

$$\begin{aligned}
\mathcal{K} &= \frac{1}{2}\int_V \rho(z)(\dot{u}_1^2 + \dot{u}_3^2)dV \\
&= \frac{1}{2}\int_0^L \Big[I_0\dot{u}_0^2 - 2I_1\dot{u}_0\dot{w}_{0,x} + I_2(\dot{w}_{0,x})^2 + 2J_1\dot{\phi}_0\dot{u}_0 - 2J_2\dot{\phi}_0\dot{w}_{0,x} + K_2\dot{\phi}_0^2 + I_0\dot{w}_0^2\Big]dx
\end{aligned} \tag{8}$$

3

where dot-superscript denotes the differentiation with respect to the time t; ρ is the mass density of each layer, and $I_0, I_1, I_2, J_1, J_2, K_2$ are the inertia coefficients defined by:

$$(I_0, I_1, I_2, J_1, J_2, K_2) = \sum_{k=1}^{n} \int_{z_k}^{z_{k+1}} \rho^{(k)}(1, z, z^2, \Psi, z\Psi, \Psi^2)bdz \tag{9}$$

The total potential energy of system is expressed by:

$$\Pi = \mathcal{U} + \mathcal{V} - \mathcal{K}$$
$$\Pi = \frac{1}{2}\int_0^L \left[A(u_{0,x})^2 - 2Bu_{0,x}w_{0,xx} + D(w_{0,xx})^2 + 2B^s u_{0,x}\phi_{0,x} - 2D^s w_{0,xx}\phi_{0,x} + H^s(\phi_{0,x})^2 + A^s\phi_0^2 \right] dx$$
$$+ \frac{1}{2}\int_0^L N_0(w_{0,x})^2 dx - \int_0^L qw_0 dx$$
$$- \frac{1}{2}\int_0^L \left[I_0\dot{u}_0^2 - 2I_1\dot{u}_0\dot{w}_{0,x} + I_2(\dot{w}_{0,x})^2 + 2J_1\dot{\phi}_0\dot{u}_0 - 2J_2\dot{\phi}_0\dot{w}_{0,x} + K_2\dot{\phi}_0^2 + I_0\dot{w}_0^2 \right] dx \tag{10}$$

Based on Ritz method [30], the displacement field in Eq. (10) is approximated in the following forms:

$$u_0(x,t) = \sum_{j=1}^{m} \psi_j(x)u_j e^{i\omega t} \tag{11a}$$

$$w_0(x,t) = \sum_{j=1}^{m} \varphi_j(x)w_j e^{i\omega t} \tag{11b}$$

$$\phi_0(x,t) = \sum_{j=1}^{m} \xi_j(x)\phi_j e^{i\omega t} \tag{11c}$$

where ω is the frequency, $i^2 = -1$ the imaginary unit; (u_j, w_j, ϕ_j) are unknown values to be determined; $\psi_j(x)$, $\varphi_j(x)$ **and** $\xi_j(x)$ **are the shape functions which are proposed for simply supported (S-S), clamped-clamped (C-C) and clamped-free (C-F) boundary conditions given in Table 1. It is clear that the proposed shape functions satisfy various boundary conditions given in Table 2. It is noted that the inappropriate shape functions may cause slow convergence rates and numerical instabilities [21, 22]. In addition, for shape functions which do not satisfy boundary conditions, Lagrangian multipliers method can be used to impose boundary conditions [24, 33, 34].**

The governing equations of motion can be obtained by substituting Eq. (11) into Eq. (10) and using Lagrange's equations:

$$\frac{\partial \Pi}{\partial q_j} - \frac{d}{dt}\frac{\partial \Pi}{\partial \dot{q}_j} = 0 \tag{12}$$

4

with q_j representing the values of (u_j, w_j, ϕ_j), that leads to:

$$\left(\begin{bmatrix} \mathbf{K}^{11} & \mathbf{K}^{12} & \mathbf{K}^{13} \\ ^T\mathbf{K}^{12} & \mathbf{K}^{22} & \mathbf{K}^{23} \\ ^T\mathbf{K}^{13} & ^T\mathbf{K}^{23} & \mathbf{K}^{33} \end{bmatrix} - \omega^2 \begin{bmatrix} \mathbf{M}^{11} & \mathbf{M}^{12} & \mathbf{M}^{13} \\ ^T\mathbf{M}^{12} & \mathbf{M}^{22} & \mathbf{M}^{23} \\ ^T\mathbf{M}^{13} & ^T\mathbf{M}^{23} & \mathbf{M}^{33} \end{bmatrix}\right) \left\{\begin{matrix} \mathbf{u} \\ \mathbf{w} \\ \phi \end{matrix}\right\} = \left\{\begin{matrix} \mathbf{0} \\ \mathbf{F} \\ \mathbf{0} \end{matrix}\right\} \tag{13}$$

where the components of stiffness matrix $\mathbf{K}$ and mass matrix $\mathbf{M}$ are given by:

$$
\begin{aligned}
K_{ij}^{11} &= A \int_0^L \psi_{i,x}\psi_{j,x}\,dx, \, K_{ij}^{12} = -B\int_0^L \psi_{i,x}\varphi_{j,xx}\,dx, \, K_{ij}^{13} = B^s \int_0^L \psi_{i,x}\xi_{j,x}\,dx \\
K_{ij}^{22} &= D\int_0^L \varphi_{i,xx}\varphi_{j,xx}\,dx + N^0 \int_0^L \varphi_{i,x}\varphi_{j,x}\,dx \\
K_{ij}^{23} &= -D^s \int_0^L \varphi_{i,xx}\xi_{j,x}\,dx, \, K_{ij}^{33} = H^s \int_0^L \xi_{i,x}\xi_{j,x}\,dx + A^s \int_0^L \xi_i\xi_j\,dx \\
M_{ij}^{11} &= I_0 \int_0^L \psi_i\psi_j\,dx, \, M_{ij}^{12} = -I_1 \int_0^L \psi_i\varphi_{j,x}\,dx, \, M_{ij}^{13} = J_1 \int_0^L \psi_i\xi_j\,dx \\
M_{ij}^{22} &= I_0 \int_0^L \varphi_i\varphi_j\,dx + I_2 \int_0^L \varphi_{i,x}\varphi_{j,x}\,dx, \, M_{ij}^{23} = -J_2 \int_0^L \varphi_{i,x}\xi_j\,dx \\
M_{ij}^{33} &= K_2 \int_0^L \xi_i\xi_j\,dx, \, F_i = \int_0^L q\varphi_i\,dx
\end{aligned}
\tag{14}
$$

The deflection, stresses, critical buckling loads and natural frequencies of composite beams can be determined by solving Eq. (13).

3. Numerical examples

In this section, convergence and verification studies are carried out to demonstrate the accuracy of the proposed solution and to investigate the responses of composite beams with various boundary conditions for bending, vibration and buckling problems. For static analysis, the beam is subjected to a uniformly distributed load with density q. Laminates are supposed to have equal thicknesses and made of the same orthotropic materials whose properties are followed:

- Material I [21]: E_1/E_2= open, $G_{12} = G_{13} = 0.6E_2, G_{23} = 0.5E_2, \nu_{12} = 0.25$

- Material II [21]: E_1/E_2= open, $G_{12} = G_{13} = 0.5E_2, G_{23} = 0.2E_2, \nu_{12} = 0.25$

- Material III [35]: E_1=144.9 GPa, E_2=9.65 GPa, $G_{12} = G_{13}$= 4.14 GPa, G_{23}=3.45 GPa, ν_{12}=0.3, ρ=1389 kg/m^3.

For convenience, the following normalized terms are used:

$$\bar{w} = \frac{100w_0 E_2 bh^3}{qL^4}, \bar{\sigma}_{xx} = \frac{bh^2}{qL^2}\sigma_{xx}\left(\frac{L}{2},\frac{h}{2}\right), \bar{\sigma}_{xz} = \frac{bh^2}{qL}\sigma_{xz}(0,0) \tag{15a}$$

$$\bar{\omega} = \frac{\omega L^2}{h}\sqrt{\frac{\rho}{E_2}} \quad \text{for Materials I and II}, \quad \bar{\omega} = \frac{\omega L^2}{h}\sqrt{\frac{\rho}{E_1}} \quad \text{for Material III} \tag{15b}$$

$$\bar{N}_{cr} = N_{cr}\frac{L^2}{E_2 bh^3} \quad \text{for Materials I and II}, \quad \bar{N}_{cr} = N_{cr}\frac{L^2}{E_1 bh^3} \quad \text{for Material III} \tag{15c}$$

In order to evaluate the convergence and reliability of the proposed solution, $(0^o/90^o/0^o)$ composite beams $(L/h=5)$ with Material I and $E_1/E_2=40$ are considered. The mid-span displacements, fundamental natural frequencies and critical buckling loads with respect to the series number m for different boundary conditions are given in Table 3. It is observed that the responses converge quickly for three boundary conditions: $m=2$ for buckling, $m=12$ for vibration, and $m=14$ for deflection. Thus, these numbers of series terms will be used for buckling, vibration and static analysis, respectively throughout the numerical examples. In comparison, the present trigonometric solution appears convergence more quickly than the polynomial series solution [33], especially for buckling analysis.

3.1. Static analysis

As the first example, $(0^o/90^o/0^o)$ and $(0^o/90^o)$ composite beams with material II and $E_1/E_2=25$ are considered. Their mid-span displacements for various boundary conditions with 5 ratios of length-to-depth, $L/h=5, 10, 20, 30, 50$ are given in Tables 4-5 and compared to earlier studies. It is observed that the present solutions are in excellent agreement with those calculated by various higher-order theories ([11], [14], [24], [36], [37]). The axial and transverse shear stresses of these beams with $L/h=5, 10, 20$ are presented in Table 6 and compared to solutions obtained by Vo and Thai [14] and Zenkour [37]. Good agreements with the previous models are also found. The variation of the axial and shear stress through the beam depth is displayed in Figure 3, in which a parabolic distribution and traction-free boundary conditions of shear stress is observed.

Next, the effect of fibre angle change on the mid-span displacements of $(\theta/-\theta)_s$ composite beams $(L/h=10)$ with material II and $E_1/E_2=25$ is plotted in Figure 2. It can be seen that the mid-span transverse displacement increases with the fibre angle, the lower curve corresponds to the C-F beams while the highest curve is C-C ones.

3.2. Vibration and buckling analysis

Tables 7-9 report the fundamental frequencies and critical buckling loads of $(0^o/90^o/0^o)$ and $(0^o/90^o)$ composite beams with different boundary conditions. The present solutions are validated

by comparison with those derived from HBTs ([11], [15], [21], [22], [24], [25], [26]). Excellent agreements between solutions from the present model and previous ones are observed while a slight deviation with those from Mantari and Canales [24] is found for L/h=5. The first three mode shapes of $(0^o/90^o/0^o)$ and $(0^o/90^o)$ composite beams (L/h=10) with material I and E_1/E_2=40 is plotted in Figure 4. It can be seen that the symmetric beam exhibits double coupled vibration (w_0, ϕ_0) whereas the anti-symmetric one presents triply coupled vibration (u_0, w_0, ϕ_0). The effect of the ratio of material anisotropy on the fundamental frequencies and critical buckling loads is plotted in Figure 5. Obviously, the results increase with E_1/E_2.

Finally, $(\theta/-\theta)_s$ composite beams (L/h=15) with material III are analysed. The effects of fibre angle variation on the fundamental frequencies and critical buckling loads are illustrated in Table 10 and Figure 6. It can be seen that the results decrease with an increase of fibre angle. A good agreement between the present solutions and those obtained from [6] is observed. It should be noted that there exist slight deviations between the present solution and Chandrashekhara et al. [6] with those from previous studies ([15], [23], [27]). $[30^o/-30^o]_s$ composite beams with S-S, C-F and C-C boundary conditions are chosen to investigate the effect of the span-to-depth ratio on the fundamental frequencies and critical buckling loads (Figure 7). It can be seen that the results increase with the increase of L/h. The effect of the span-to-depth ratio is effectively significant for C-C boundary condition when $L/h \leq$20.

4. Conclusions

The authors proposed a new analytical solution for static, buckling and vibration of laminated composite beams based on a higher-order beam theory. This solution based on trigonometric series are developed for various boundary conditions. Numerical results are obtained to compare with previous studies and to investigate effects of fibre angle and material anisotropy on the deflections, stresses, natural frequencies, critical buckling loads and corresponding mode shapes. The obtained results showed that the proposed series solution converges quickly for buckling analysis. The present solution is found to simple and efficient in analysis of laminated composite beams with various boundary conditions.

Acknowledgements

References

[1] Y. M. Ghugal, R. P. Shimpi, A review of refined shear deformation theories for isotropic and anisotropic laminated beams, Journal of Reinforced Plastics and Composites 20 (3) (2001) 255–272.

[2] R. Aguiar, F. Moleiro, C. M. Soares, Assessment of mixed and displacement-based models for static analysis of composite beams of different cross-sections, Composite Structures 94 (2) (2012) 601 – 616.

[3] W. Zhen, C. Wanji, An assessment of several displacement-based theories for the vibration and stability analysis of laminated composite and sandwich beams, Composite Structures 84 (4) (2008) 337 – 349.

[4] F.-G. Yuan, R. E. Miller, A higher order finite element for laminated beams, Composite Structures 14 (2) (1990) 125 – 150.

[5] H. Yu, A higher-order finite element for analysis of composite laminated structures, Composite Structures 28 (4) (1994) 375 – 383.

[6] K. Chandrashekhara, K. Bangera, Free vibration of composite beams using a refined shear flexible beam element, Computers & Structures 43 (4) (1992) 719 – 727.

[7] S. Marur, T. Kant, Free vibration analysis of fiber reinforced composite beams using higher order theories and finite element modelling, Journal of Sound and Vibration 194 (3) (1996) 337 – 351.

[8] M. Karama, B. A. Harb, S. Mistou, S. Caperaa, Bending, buckling and free vibration of laminated composite with a transverse shear stress continuity model, Composites Part B: Engineering 29 (3) (1998) 223 – 234.

[9] G. Shi, K. Lam, T. Tay, On efficient finite element modeling of composite beams and plates using higher-order theories and an accurate composite beam element, Composite Structures 41 (2) (1998) 159 – 165.

[10] G. Shi, K. Lam, Finite element vibration analysis of composite beams based on higher-order beam theory, Journal of Sound and Vibration 219 (4) (1999) 707 – 721.

[11] M. Murthy, D. R. Mahapatra, K. Badarinarayana, S. Gopalakrishnan, A refined higher order finite element for asymmetric composite beams, Composite Structures 67 (1) (2005) 27 – 35.

[12] P. Subramanian, Dynamic analysis of laminated composite beams using higher order theories and finite elements, Composite Structures 73 (3) (2006) 342 – 353.

[13] P. Vidal, O. Polit, A family of sinus finite elements for the analysis of rectangular laminated beams, Composite Structures 84 (1) (2008) 56 – 72.

[14] T. P. Vo, H.-T. Thai, Static behavior of composite beams using various refined shear deformation theories, Composite Structures 94 (8) (2012) 2513 – 2522.

[15] T. P. Vo, H.-T. Thai, Vibration and buckling of composite beams using refined shear deformation theory, International Journal of Mechanical Sciences 62 (1) (2012) 67 – 76.

[16] J. Mantari, F. Canales, Finite element formulation of laminated beams with capability to model the thickness expansion, Composites Part B: Engineering 101 (2016) 107 – 115.

[17] J. Li, Z. Wu, X. Kong, X. Li, W. Wu, Comparison of various shear deformation theories for free vibration of laminated composite beams with general lay-ups, Composite Structures 108 (2014) 767 – 778.

[18] H. MATSUNAGA, Vibration and buckling of multilayered composite beams according to higher order deformation theories, Journal of Sound and Vibration 246 (1) (2001) 47 – 62.

[19] J. Mantari, F. Canales, A unified quasi-3d {HSDT} for the bending analysis of laminated beams, Aerospace Science and Technology 54 (2016) 267 – 275.

[20] T. Kant, S. Marur, G. Rao, Analytical solution to the dynamic analysis of laminated beams using higher order refined theory, Composite Structures 40 (1) (1997) 1 – 9.

[21] M. Aydogdu, Vibration analysis of cross-ply laminated beams with general boundary conditions by ritz method, International Journal of Mechanical Sciences 47 (11) (2005) 1740 – 1755.

[22] M. Aydogdu, Buckling analysis of cross-ply laminated beams with general boundary conditions by ritz method, Composites Science and Technology 66 (10) (2006) 1248 – 1255.

[23] M. Aydogdu, Free vibration analysis of angle-ply laminated beams with general boundary conditions, Journal of Reinforced Plastics and Composites 25 (15) (2006) 1571–1583.

[24] J. Mantari, F. Canales, Free vibration and buckling of laminated beams via hybrid ritz solution for various penalized boundary conditions, Composite Structures 152 (2016) 306 – 315.

[25] A. Khdeir, J. Reddy, Free vibration of cross-ply laminated beams with arbitrary boundary conditions, International Journal of Engineering Science 32 (12) (1994) 1971 – 1980.

[26] A. Khdeir, J. Redd, Buckling of cross-ply laminated beams with arbitrary boundary conditions, Composite Structures 37 (1) (1997) 1 – 3.

[27] W. Chen, C. Lv, Z. Bian, Free vibration analysis of generally laminated beams via state-space-based differential quadrature, Composite Structures 63 (34) (2004) 417 – 425.

[28] L. Jun, L. Xiaobin, H. Hongxing, Free vibration analysis of third-order shear deformable composite beams using dynamic stiffness method, Archive of Applied Mechanics 79 (12) (2009) 1083–1098.

[29] L. Jun, H. Hongxing, Free vibration analyses of axially loaded laminated composite beams based on higher-order shear deformation theory, Meccanica 46 (6) (2011) 1299–1317.

[30] J. N. Reddy, Mechanics of Laminated Composites Plates: Theory and Analysis, CRC Press, Boca Raton, 1997.

[31] E. Reissner, On transverse bending of plates, including the effect of transverse shear deformation, International Journal of Solids and Structures 11 (5) (1975) 569 – 573.

[32] K. Soldatos, T. Timarci, A unified formulation of laminated composite, shear deformable, five-degrees-of-freedom cylindrical shell theories, Composite Structures 25 (1) (1993) 165 – 171.

[33] T.-K. Nguyen, T. T.-P. Nguyen, T. P. Vo, H.-T. Thai, Vibration and buckling analysis of functionally graded sandwich beams by a new higher-order shear deformation theory, Composites Part B: Engineering 76 (2015) 273 – 285.

[34] T.-K. Nguyen, T. P. Vo, B.-D. Nguyen, J. Lee, An analytical solution for buckling and vibration analysis of functionally graded sandwich beams using a quasi-3d shear deformation theory, Composite Structures (2015) –doi:http://dx.doi.org/10.1016/j.compstruct.2015.11.074.

[35] K. Chandrashekhara, K. Krishnamurthy, S. Roy, Free vibration of composite beams including rotary inertia and shear deformation, Composite Structures 14 (4) (1990) 269 – 279.

[36] A. Khdeir, J. Reddy, An exact solution for the bending of thin and thick cross-ply laminated beams, Composite Structures 37 (2) (1997) 195 – 203.

[37] A. M. Zenkour, Transverse shear and normal deformation theory for bending analysis of laminated and sandwich elastic beams, Mechanics of Composite Materials and Structures 6 (3) (1999) 267–283.

CAPTIONS OF TABLES

Table 1: Trigonometric series for shape functions.

Table 2: Three different boundary conditions of beams.

Table 3: Convergence studies for normalized mid-span displacements, fundamental frequencies and critical buckling loads of $(0^o/90^o/0^o)$ composite beams ($L/h = 5$, Material I, $E_1/E_2 = 40$).

Table 4: Normalized mid-span displacements of $(0^o/90^o/0^o)$ composite beam under a uniformly distributed load (Material II, E_1/E_2=25).

Table 5: Normalized mid-span displacements of $(0^o/90^o)$ composite beams under a uniformly distributed load (Material II, E_1/E_2=25).

Table 6: Normalized stresses of $(0^o/90^o/0^o)$ and $(0^o/90^o)$ composite beams with simply-supported boundary conditions (Material II, E_1/E_2=25).

Table 7: Normalized fundamental frequencies of $(0^o/90^o/0^o)$ and $(0^o/90^o)$ composite beams (Material I, E_1/E_2=40).

Table 8: Normalized critical buckling loads of $(0^o/90^o/0^o)$ and $(0^o/90^o)$ composite beams with simply-supported boundary conditions (Materials I and II, E_1/E_2=10).

Table 9: Normalized critical buckling loads of $(0^o/90^o/0^o)$ and $(0^o/90^o)$ composite beams (Material I, E_1/E_2=40).

Table 10: Normalized fundamental frequencies of $[\theta/-\theta]_s$ composite beams with respect to the fibre angle change (L/h=15, Materials III).

12

CAPTIONS OF FIGURES

Figure 1: Geometry of laminated composite beams.

Figure 2: Effects of the fibre angle change on the normalized transverse displacement of $[\theta/-\theta]_s$ composite beams (L/h=10, Material II, E_1/E_2=25).

Figure 3: Distribution of the normalized stresses ($\bar{\sigma}_{xx}$, $\bar{\sigma}_{xz}$) through the beam depth of ($0^o/90^o/0^o$) and ($0^o/90^o$) composite beams with simply-supported boundary conditions (Material II, E_1/E_2=25).

Figure 4: The first three mode shapes of ($0^o/90^o/0^o$) and ($0^o/90^o$) composite beams with simply-supported boundary conditions (L/h=10, Material I, E_1/E_2=40).

Figure 5: Effects of material anisotropy on the normalized fundamental frequencies and critical buckling loads of ($0^o/90^o/0^o$) and ($0^o/90^o$) composite beams with simply-supported boundary conditions (L/h=10, Material I).

Figure 6: Effects of the fibre angle change on the normalized fundamental frequencies and critical buckling loads of $[\theta/-\theta]_s$ composite beams (L/h=15, Material III).

Figure 7: Effects of the span-to-depth ratio on the normalized fundamental frequencies and critical buckling loads of $[30^o/\text{-}30^o]_s$ composite beams (L/h=15, Material III).

Table 1: Trigonometric series for shape functions.

Boundary conditions	$\varphi_j(x)$	$\psi_j(x)$	$\xi_j(x)$
S-S	$\sin \frac{j\pi}{L}x$	$\cos \frac{j\pi}{L}x$	$\cos \frac{j\pi}{L}x$
C-F	$1 - \cos \frac{(2j-1)\pi}{2L}x$	$\sin \frac{(2j-1)\pi}{2L}x$	$\sin \frac{(2j-1)\pi}{2L}x$
C-C	$\sin^2 \frac{j\pi}{L}x$	$\sin \frac{2j\pi}{L}x$	$\sin \frac{2j\pi}{L}x$

Table 2: Three different boundary conditions of beams.

BC	$x = 0$	$x = L$
S-S	$w_0 = 0$	$w_0 = 0$
C-F	$u_0 = 0,\ w_0 = 0,\ \phi_0 = 0,\ w_{0,x} = 0$	
C-C	$u_0 = 0,\ w_0 = 0,\ \phi_0 = 0,\ w_{0,x} = 0$	$u_0 = 0,\ w_0 = 0,\ \phi_0 = 0,\ w_{0,x} = 0$

Table 3: Convergence studies for normalized mid-span displacements, fundamental frequencies and critical buckling loads of $(0^o/90^o/0^o)$ composite beams ($L/h = 5$, Material I, $E_1/E_2 = 40$).

BC	Number of series (m)							
	2	4	6	8	10	12	14	16
Deflection								
S-S	1.4978	1.4632	1.4685	1.4671	1.4676	1.4674	1.4675	1.4674
C-F	3.6160	4.0311	4.1035	4.1380	4.1499	4.1571	4.1604	4.1626
C-C	0.8696	0.9183	0.9274	0.9301	0.9311	0.9316	0.9319	0.9320
Fundamental frequency								
S-S	9.2084	9.2084	9.2084	9.2084	9.2084	9.2084	9.2084	9.2084
C-F	4.3499	4.2691	4.2473	4.2394	4.2359	4.2342	4.2332	4.2327
C-C	11.8716	11.6673	11.6269	11.6143	11.6093	11.6069	11.6056	11.6048
Critical buckling load								
S-S	8.6132	8.6132	8.6132	8.6132	8.6132	8.6132	8.6132	8.6132
C-F	4.7080	4.7080	4.7080	4.7080	4.7080	4.7080	4.7080	4.7080
C-C	11.6518	11.6518	11.6518	11.6518	11.6518	11.6518	11.6518	11.6518

Table 4: Normalized mid-span displacements of $(0^o/90^o/0^o)$ composite beam under a uniformly distributed load (Material II, E_1/E_2=25).

BC	Theory	L/h				
		5	10	20	30	50
S-S	Present	2.412	1.096	0.759	0.697	0.665
	Murthy et al. [11]	2.398	1.090	-	-	0.661
	Khdeir and Reddy [36]	2.412	1.096	-	-	0.665
	Vo and Thai (HBT) [14]	2.414	1.098	0.761	-	0.666
	Zenkour [37]	2.414	1.098	-	-	0.666
	Mantari and Canales [24]	-	1.097	-	-	-
C-F	Present	6.813	3.447	2.520	2.342	2.250
	Murthy et al. [11]	6.836	3.466	-	-	2.262
	Khdeir and Reddy [36]	6.824	3.455	-	-	2.251
	Vo and Thai (HBT) [14]	6.830	3.461	2.530	-	2.257
	Mantari and Canales [24]	-	3.459	-	-	-
C-C	Present	1.536	0.531	0.236	0.177	0.147
	Khdeir and Reddy [36]	1.537	0.532	-	-	0.147
	Mantari and Canales [24]	-	0.532	-	-	-

Table 5: Normalized mid-span displacements of $(0^o/90^o)$ composite beams under a uniformly distributed load (Material II, E_1/E_2=25).

BC	Theory	L/h				
		5	10	20	30	50
S-S	Present	4.777	3.688	3.413	3.362	3.336
	Murthy et al. [11]	4.750	3.668	-	-	3.318
	Khdeir and Reddy [36]	4.777	3.688	-	-	3.336
	Vo and Thai (HBT) [14]	4.785	3.696	3.421	-	3.344
	Zenkour [37]	4.788	3.697	-	-	3.344
	Mantari and Canales [24]	-	3.731	-	-	-
C-F	Present	15.260	12.330	11.556	11.410	11.335
	Murthy et al. [11]	15.334	12.398	-	-	11.392
	Khdeir and Reddy [36]	15.279	12.343	-	-	11.337
	Vo and Thai (HBT) [14]	15.305	12.369	11.588	-	11.363
	Mantari and Canales [24]	-	12.475	-	-	-
C-C	Present	1.920	1.004	0.752	0.704	0.679
	Khdeir and Reddy [36]	1.922	1.005	-	-	0.679
	Mantari and Canales [24]	-	1.010	-	-	-

Table 6: Normalized stresses of $(0^o/90^o/0^o)$ and $(0^o/90^o)$ composite beams with simply-supported boundary conditions (Material II, E_1/E_2=25).

Lay-ups	Theory	$\bar{\sigma}_{xx}$			$\bar{\sigma}_{xz}$		
		L/h=5	10	20	L/h=5	10	20
$(0^o/90^o/0^o)$	Present	1.0696	0.8516	0.7965	0.4050	0.4289	0.4388
	Zenkour [37]	1.0669	0.8500	-	0.4057	0.4311	-
	Vo and Thai (HBT) [14]	1.0670	0.8503	0.7961	0.4057	0.4311	0.4438
$(0^o/90^o)$	Present	0.2362	0.2343	0.2338	0.9174	0.9483	0.9594
	Zenkour [37]	0.2362	0.2343	-	0.9211	0.9572	-
	Vo and Thai (HBT) [14]	0.2361	0.2342	0.2337	0.9187	0.9484	0.9425

Table 7: Normalized fundamental frequencies of $(0^o/90^o/0^o)$ and $(0^o/90^o)$ composite beams (Material I, E_1/E_2=40).

BC	Lay-ups	Theory	L/h				
			5	10	20	30	50
S-S	$(0^o/90^o/0^o)$	Present	9.208	13.614	16.338	17.055	17.462
		Murthy et al. [11]	9.207	13.611	-	-	-
		Khdeir and Reddy [25]	9.208	13.614	-	-	-
		Aydogdu [21]	9.207	-	16.337	-	-
		Vo and Thai [15]	9.206	13.607	16.327	-	17.449
		Mantari and Canales [24]	9.208	13.610	-	-	-
	$(0^o/90^o)$	Present	6.128	6.945	7.219	7.274	7.302
		Murthy et al. [11]	6.045	6.908	-	-	-
		Khdeir and Reddy [25]	6.128	6.945	-	-	-
		Aydogdu [21]	6.144	-	7.218	-	-
		Vo and Thai [15]	6.058	6.909	7.204	-	7.296
		Mantari and Canales [24]	6.109	6.913	-	-	-
C-F	$(0^o/90^o/0^o)$	Present	4.234	5.498	6.070	6.198	6.267
		Murthy et al. [11]	4.230	5.491	-	-	-
		Khdeir and Reddy [25]	4.234	5.495	-	-	-
		Aydogdu [21]	4.234	-	6.070	-	-
		Mantari and Canales [24]	4.221	5.490	-	-	-
	$(0^o/90^o)$	Present	2.383	2.543	2.591	2.600	2.605
		Murthy et al. [11]	2.378	2.541	-	-	-
		Khdeir and Reddy [25]	2.386	2.544	-	-	-
		Aydogdu [21]	2.384	-	2.590	-	-
		Mantari and Canales [24]	2.375	2.532	-	-	-
C-C	$(0^o/90^o/0^o)$	Present	11.607	19.728	29.695	34.268	37.679
		Murthy et al. [11]	11.602	19.719	-	-	-
		Khdeir and Reddy [25]	11.603	19.712	-	-	-
		Aydogdu [21]	11.637	-	29.926	-	-
		Mantari and Canales [24]	11.486	19.652	-	-	-
	$(0^o/90^o)$	Present	10.027	13.670	15.661	16.154	16.429
		Murthy et al. [11]	10.011	13.657	-	-	-
		Khdeir and Reddy [25]	10.026	13.660	-	-	-
		Aydogdu [21]	10.102	-	15.688	-	-
		Mantari and Canales [24]	9.974	13.628	-	-	-

Table 8: Normalized critical buckling loads of $(0^o/90^o/0^o)$ and $(0^o/90^o)$ composite beams with simply-supported boundary conditions (Materials I and II, $E_1/E_2=10$).

Lay-ups	Theory	L/h				
		5	10	20	30	50
Material I						
$(0^o/90^o/0^o)$	Present	4.727	6.814	7.666	7.848	7.945
	Aydogdu [22]	4.726	-	7.666	-	-
	Vo and Thai [15]	4.709	6.778	7.620	-	7.896
$(0^o/90^o)$	Present	1.920	2.168	2.241	2.255	2.262
	Aydogdu [22]	1.919	-	2.241	-	-
	Vo and Thai [15]	1.910	2.156	2.228	-	2.249
Material II						
$(0^o/90^o/0^o)$	Present	3.728	6.206	7.460	7.751	7.909
	Aydogdu [22]	3.728	-	7.459	-	-
	Vo and Thai [15]	3.717	6.176	7.416	-	7.860
$(0^o/90^o)$	Present	1.766	2.116	2.227	2.249	2.260
	Aydogdu [22]	1.765	-	2.226	-	-
	Vo and Thai [15]	1.758	2.104	2.214	-	2.247

Table 9: Normalized critical buckling loads of $(0^o/90^o/0^o)$ and $(0^o/90^o)$ composite beams (Material I, $E_1/E_2=40$).

BC	Lay-ups	Theory	L/h				
			5	10	20	30	50
S-S	$(0^o/90^o/0^o)$	Present	8.613	18.832	27.086	29.496	30.906
		Mantari and Canales [24]	8.585	18.796	-	-	-
		Khdeir and Reddy [26]	8.613	18.832	-	-	-
	$(0^o/90^o)$	Present	3.907	4.942	5.297	5.369	5.406
		Aydogdu [22]	3.906	-	-	-	-
		Mantari and Canales [24]	3.856	4.887	-	-	-
C-F	$(0^o/90^o/0^o)$	Present	4.708	6.772	7.611	7.790	7.886
		Mantari and Canales [24]	4.673	6.757	-	-	-
		Khdeir and Reddy [26]	4.708	6.772	-	-	-
	$(0^o/90^o)$	Present	1.236	1.324	1.349	1.353	1.356
		Aydogdu [22]	1.235	-	-	-	-
		Mantari and Canales [24]	1.221	1.311	-	-	-
C-C	$(0^o/90^o/0^o)$	Present	11.652	34.453	75.328	97.248	114.398
		Mantari and Canales [24]	11.502	34.365	-	-	-
		Khdeir and Reddy [26]	11.652	34.453	-	-	-
	$(0^o/90^o)$	Present	8.674	15.626	19.768	20.780	21.372
		Mantari and Canales [24]	8.509	15.468	-	-	-

Table 10: Normalized fundamental frequencies of $[\theta/-\theta]_s$ composite beams with respect to the fibre angle change (L/h=15, Materials III).

BC	Theory	Fibre angle						
		0°	15°	30°	45°	60°	75°	90°
C-C	Present	4.9116	4.7173	4.1307	3.1973	2.2019	1.6825	1.6205
	Aydogdu [23]	4.9730	4.2940	2.1950	1.9290	1.6690	1.6120	1.6190
	Chandrashekhara et al. [6]	4.8487	4.6635	4.0981	3.1843	2.1984	1.6815	1.6200
	Chen et al. [27]	4.8575	3.6484	2.3445	1.8383	1.6711	1.6161	1.6237
	Vo and Thai [15]	4.8969	4.5695	3.2355	1.9918	1.6309	1.6056	1.6152
S-S	Present	2.6563	2.5108	2.1033	1.5367	1.0121	0.7608	0.7317
	Aydogdu [23]	2.6510	1.8960	1.1410	0.8040	0.7360	0.7250	0.7290
	Chandrashekhara et al. [6]	2.6560	2.5105	2.1032	1.5368	1.0124	0.7611	0.7320
	Vo and Thai [15]	2.6494	2.4039	1.5540	0.9078	0.7361	0.7247	0.7295
C-F	Present	0.9832	0.9259	0.7683	0.5553	0.3631	0.2722	0.2618
	Aydogdu [23]	0.9810	0.6760	0.4140	0.2880	0.2620	0.2580	0.2600
	Chandrashekhara et al. [6]	0.9820	0.9249	0.7678	0.5551	0.3631	0.2723	0.2619
	Vo and Thai [15]	0.9801	0.8836	0.5614	0.3253	0.2634	0.2593	0.2611
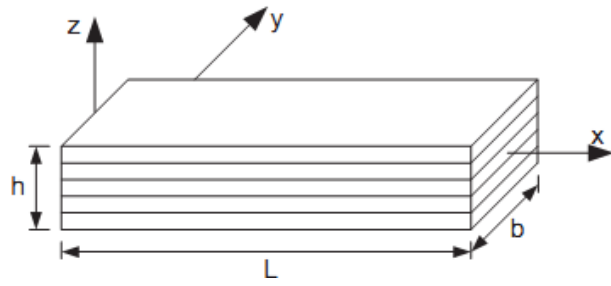
Figure 1: Geometry of laminated composite beams.
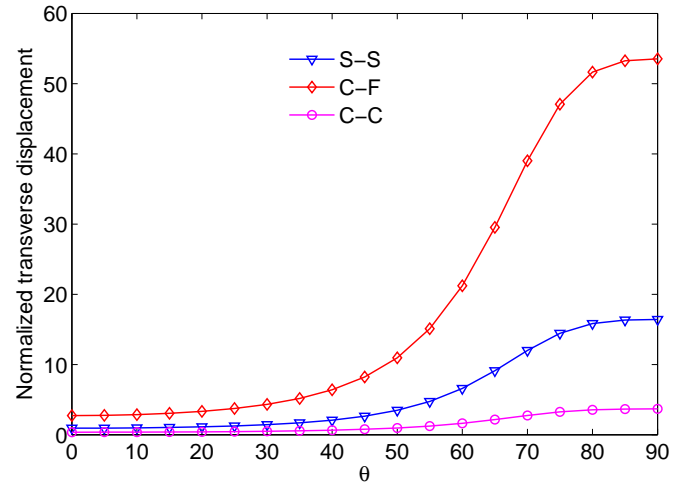
Figure 2: Effects of the fibre angle change on the normalized transverse displacement of $[\theta/-\theta]_s$ composite beams (L/h=10, Material II, E_1/E_2=25).

(a) $(0^o/90^o/0^o)$
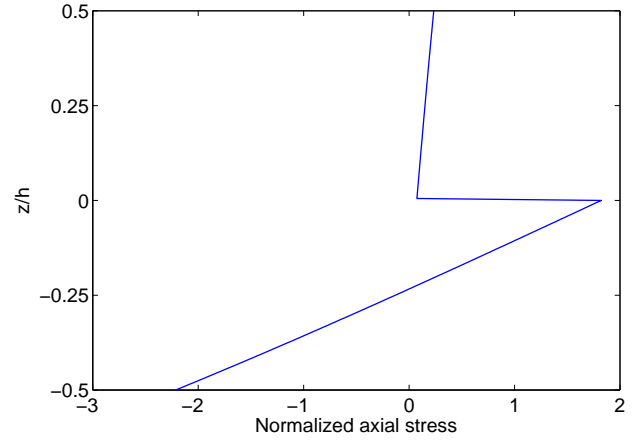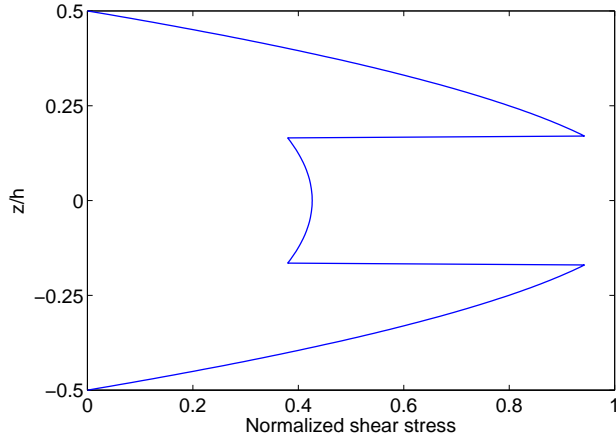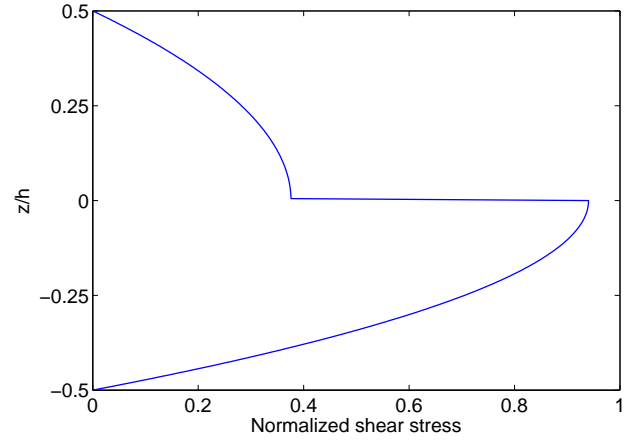
(b) $(0^o/90^o)$

(c) $(0^o/90^o/0^o)$

(d) $(0^o/90^o)$

Figure 3: Distribution of the normalized stresses $(\bar{\sigma}_{xx}, \bar{\sigma}_{xz})$ through the beam depth of $(0^o/90^o/0^o)$ and $(0^o/90^o)$ composite beams with simply-supported boundary conditions (Material II, $E_1/E_2=25$).

(a) Mode 1, $\bar{\omega}_1$=13.6136 $(0^o/90^o/0^o)$

(b) Mode 1, $\bar{\omega}_1$=6.9451 $(0^o/90^o)$

(c) Mode 2, $\bar{\omega}_2$=36.8334 $(0^o/90^o/0^o)$

(d) Mode 2, $\bar{\omega}_2$=24.5139 $(0^o/90^o)$

(e) Mode 3, $\bar{\omega}_3$=60.8686 $(0^o/90^o/0^o)$

(f) Mode 3, $\bar{\omega}_3$=47.5396 $(0^o/90^o)$

Figure 4: The first three mode shapes of $(0^o/90^o/0^o)$ and $(0^o/90^o)$ composite beams with simply-supported boundary conditions (L/h=10, Material I, E_1/E_2=40).

Figure 5: Effects of material anisotropy on the normalized fundamental frequencies and critical buckling loads of $(0^o/90^o/0^o)$ and $(0^o/90^o)$ composite beams with simply-supported boundary conditions (L/h=10, Material I).
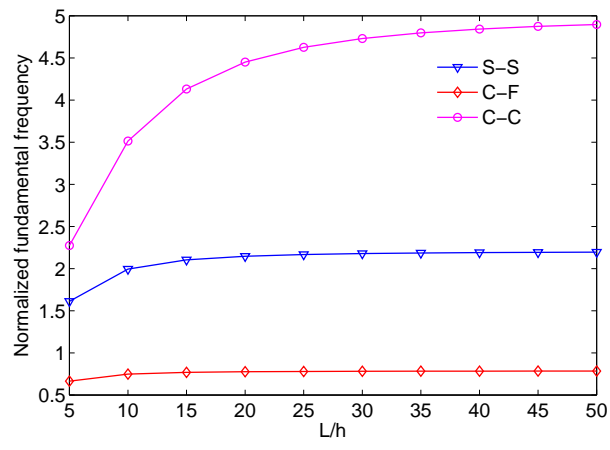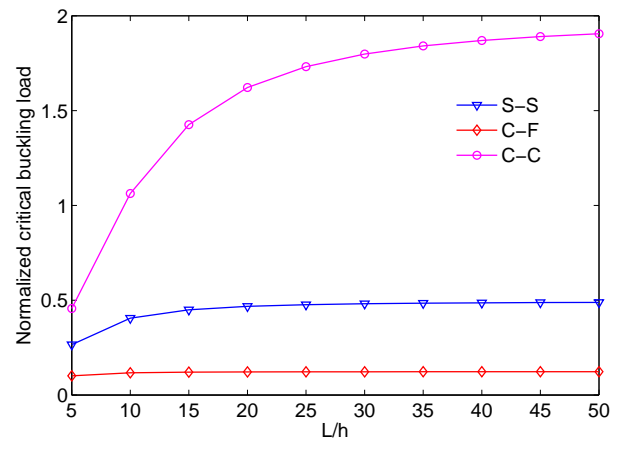
Figure 6: Effects of the fibre angle change on the normalized fundamental frequencies and critical buckling loads of $[\theta/-\theta]_s$ composite beams (L/h=15, Material III).

Figure 7: Effects of the span-to-depth ratio on the normalized fundamental frequencies and critical buckling loads of $[30^o/\text{-}30^o]_s$ composite beams (L/h=15, Material III).